Supplementary Figures.

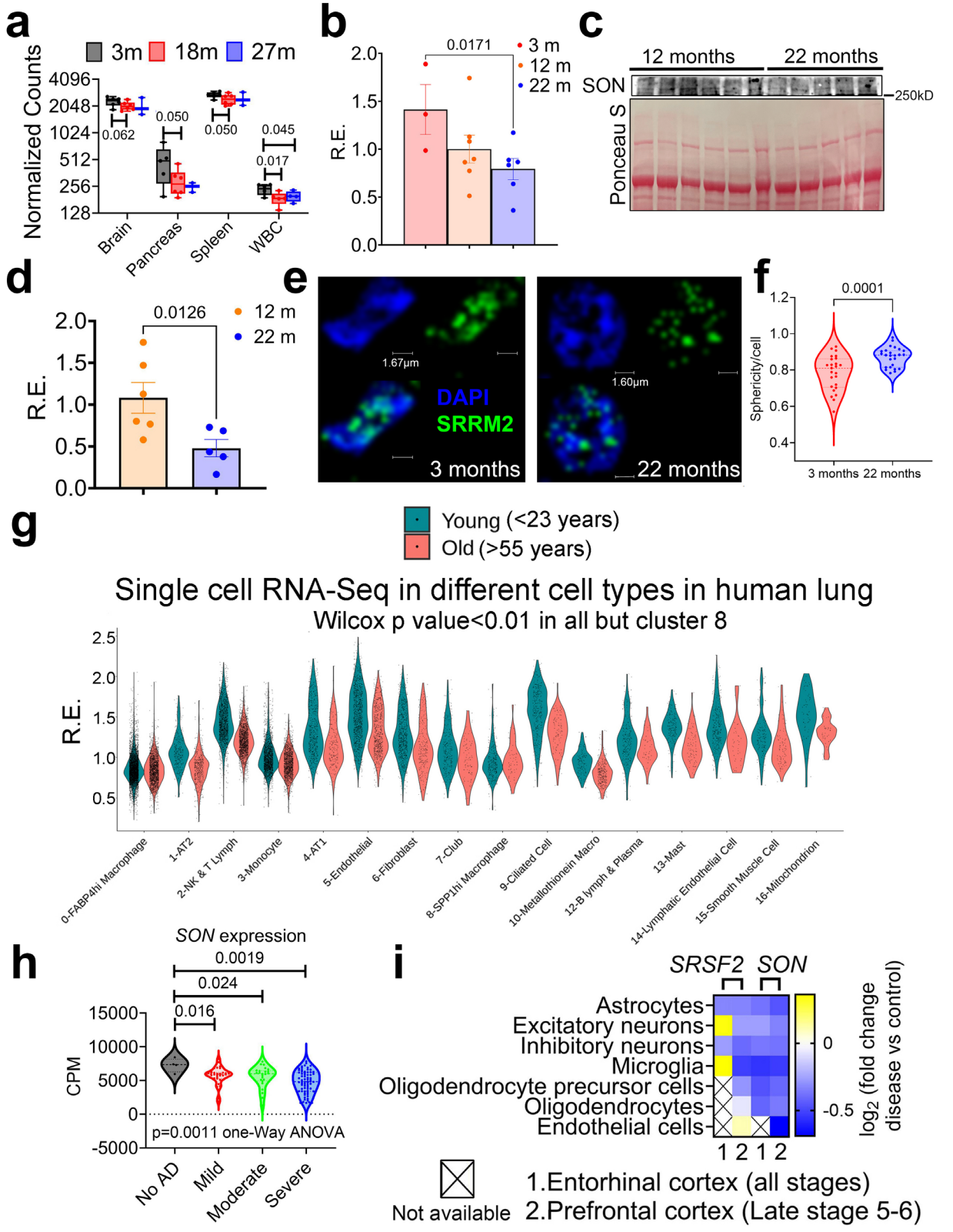

Supplementary Figure 1. SON expression is reduced during aging in mice and humans. (**a**) Normalized counts of *Son* mRNA in different mouse tissues with different ages (WBC; White blood

cells) according to Tabula Muris Senis database (n=3~6) [132, 133]. (**b**) qPCR of *Son* level in liver of mice with different ages (n=3~7). (**c, d**) Western blot (**c**) and quantification (**d**) of SON level in liver of mice with different ages (n=5~6). (**e, f**) Representative immunofluorescence images of SRRM2 and DAPI in the liver of 3 and 22 months old male mice (**e**) and quantification of the sphericity of nuclear speckles (**f**). n=25 for both age groups. (**g**) Single cell RNA-seq data of *SON* mRNA level in different cell types in lung tissues of young and aging humans, reported from [20]. (**h**) Counts per million normalized expressions of *SON* in brains of human AD compiled from RNA-seq data from the AMP-AD consortium. (**i**) Heat map showing relative expression of *SRSF2* and *SON* in different cell types in the cortex of human AD subjects [134]. Blue color indicates lower level in AD subjects compared to controls. Data: Mean ± S.E.M. Statistical tests used: two-way ANOVA and Turkey multiple comparison for h, unpaired one-tailed Student's t-test for a, b, d, and f. Wilcoxon test for g.

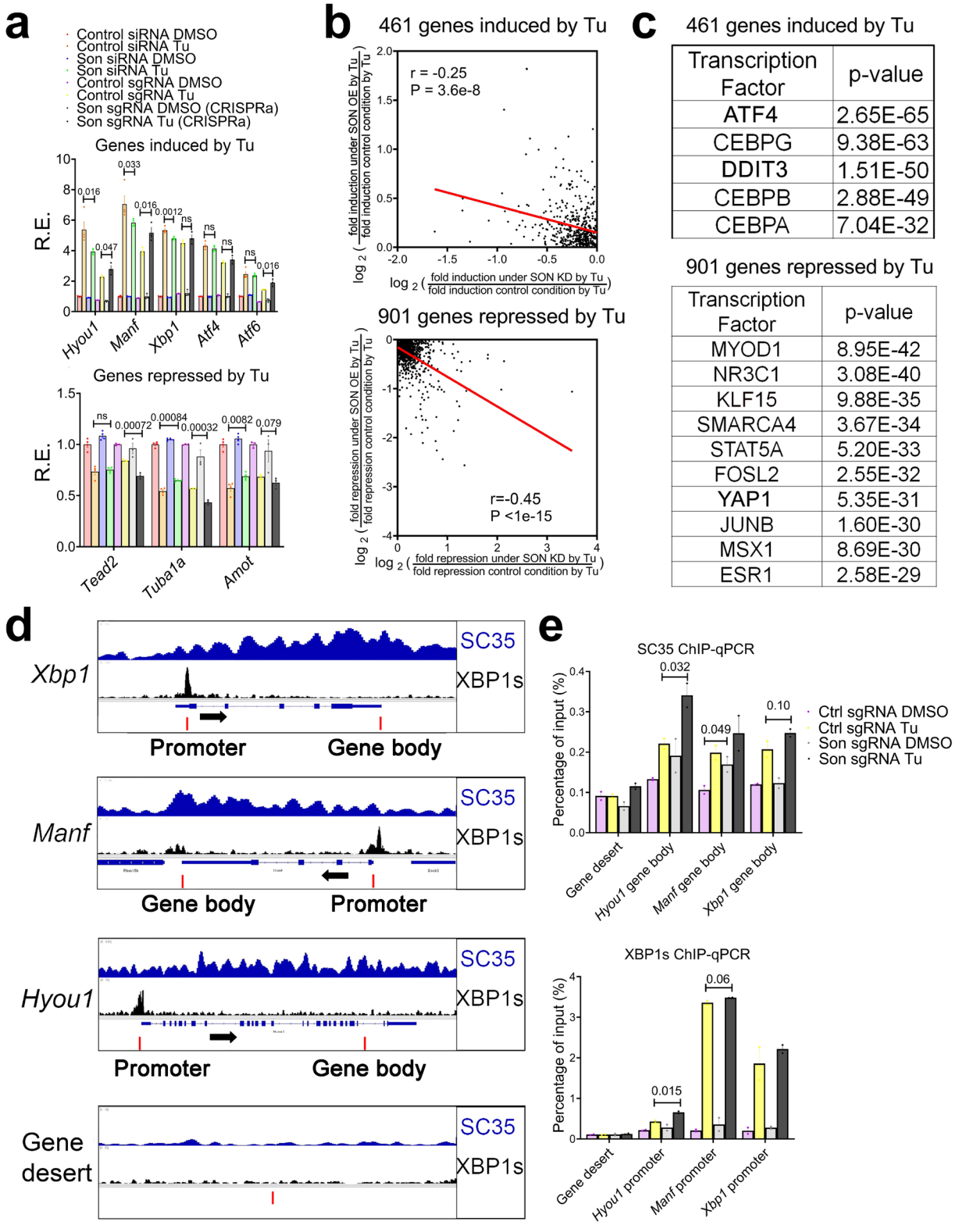

Supplementary Figure 2. Genetic rejuvenation of nuclear speckles by SON. (**a**) Relative expression (R.E.) of representative proteostasis genes (top) and YAP1 target genes (bottom) in

response to Tu in the presence of SON OE/KD (n=4 for SON KD and n=3 for SON OE). (**b**) Scatter plot showing relative fold change by *Son* KD versus SON OE for both Tu-induced and Tu-repressed genes. (**c**) Top predicted transcription regulators of 461 and 901 genes by the LISA Cistrome DB TR ChIP-Seq models. (**d, e**) Selected genes aligned for SC35 and XBP1s ChIP-seq signal from CT12 in XBP1^{Flox} mice [6] (**d**) and ChIP-qPCR of XBP1s and SC35 on selected regions (indicated by red bars) (n=2) (**e**). Data: Mean ± S.E.M. Statistical tests used: unpaired one-tailed Student's t-test for a and e. Linear regression for b.

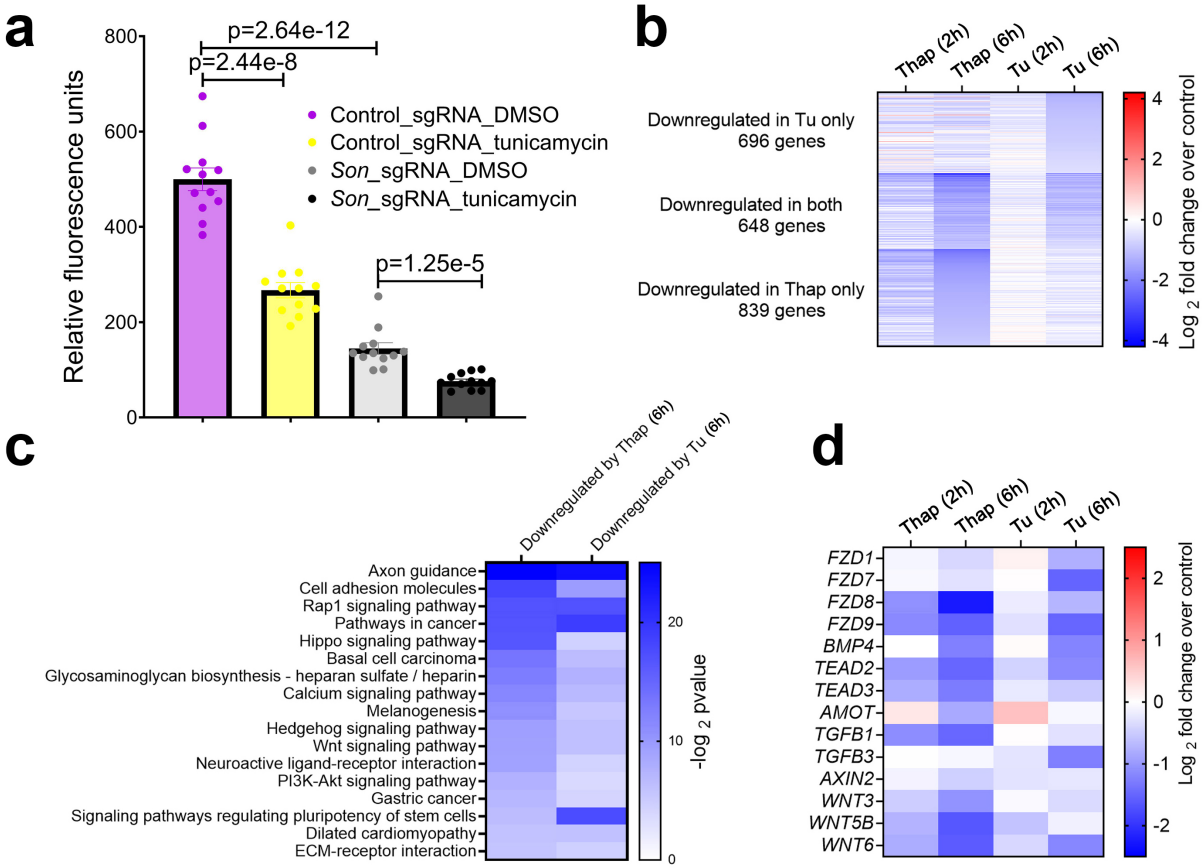

1766

1767 **Supplementary Figure 3. YAP1 transcriptional output is repressed during ER stress.** (**a**)
1768 TEAD luciferase reporter assay in control and SON OE MEFs in response to Tu (n=12 for all
1769 groups). (**b**) Heatmap showing transcriptomes that are significantly downregulated (log $_2$-fold
1770 change smaller than -0.5) with a p value less than 0.05) either under Tu or Thap treatment at 6h.
1771 (**c**) GO analysis of genes that are significantly downregulated either under Tu or Thap treatment
1772 at 6h. (**d**) Heatmap of representative YAP1 target genes as in **b**. Data: Mean ± S.E.M. Statistical
1773 tests used: unpaired one-tailed Student's t-test for a.

1774

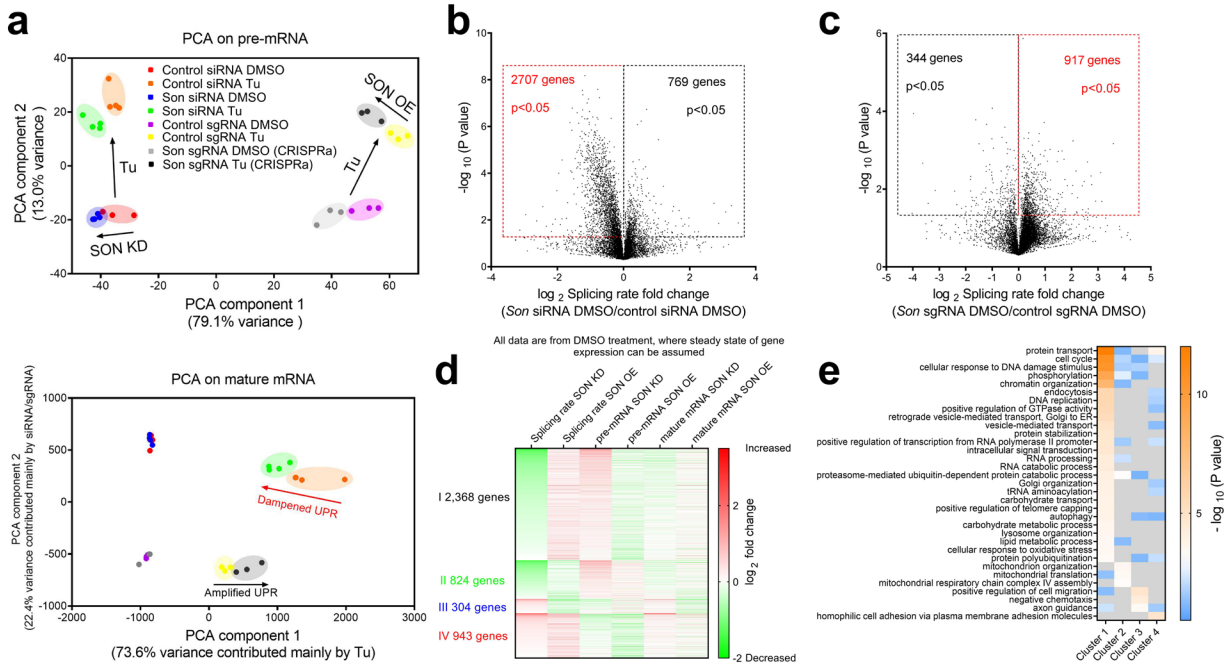

Supplementary Figure 4. SON regulates mRNA splicing rates under both basal and ER stress conditions (**a**) PCA analysis of global transcriptional response to Tu in the presence of SON OE/KD. Both pre-mRNA (top) and mature mRNA (bottom) are shown. (**b, c**) Volcano plot of mRNA splicing rates changes in SON KD (**b**) or OE (**c**) MEFs under basal condition (DMSO). (**d**) Heat map of fold change of RNA splicing rate, pre and mature mRNA level in SON OE/KD MEFs compared to control MEFs under vehicle (DMSO) condition. Four clusters of genes are shown. (**e**) GO analysis of genes in four clusters showing enriched KEGG pathways.

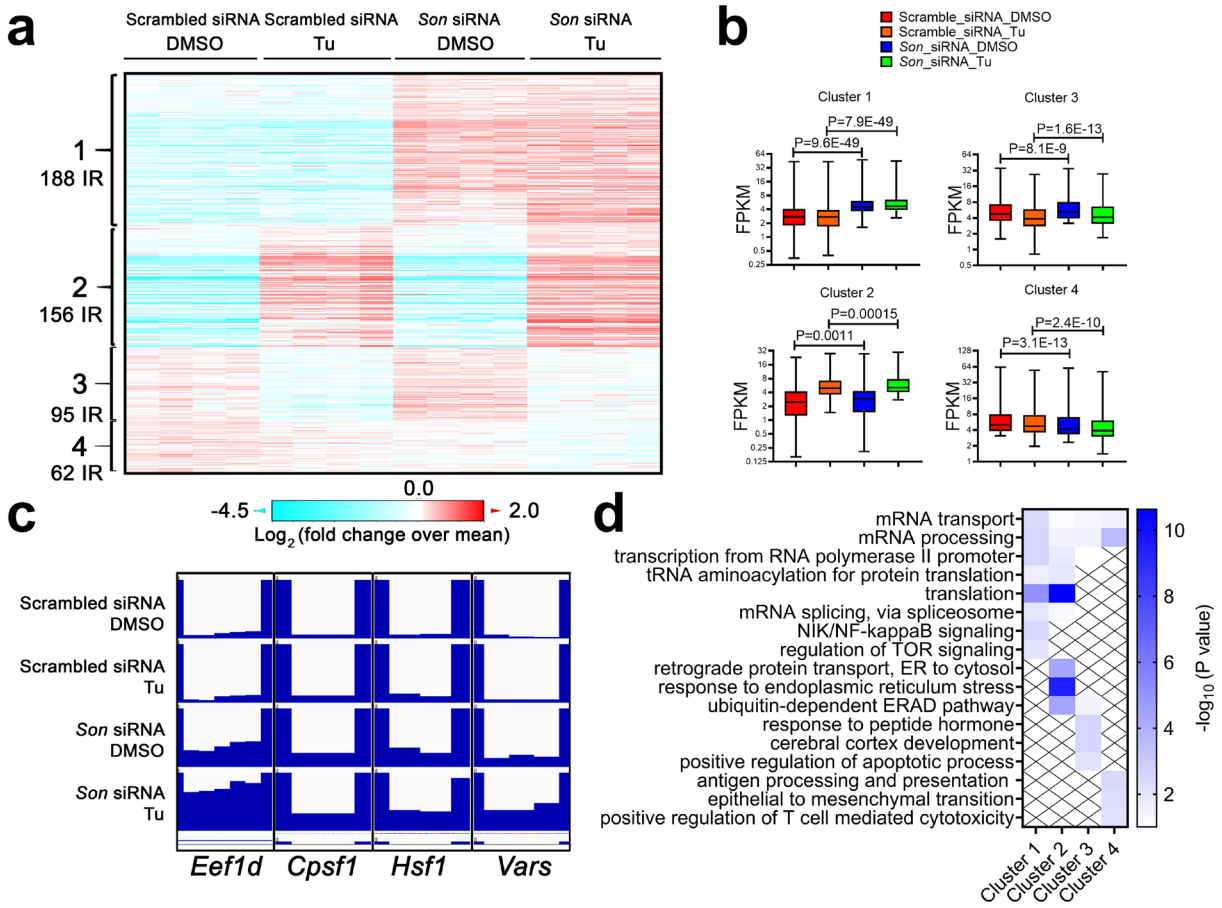

Supplementary Figure 5. SON knockdown increases intron retention of proteostasis and mRNA metabolism genes. Heat map (**a**) and quantification (**b**) of intron retention events in MEFs with control or SON KD under basal (DMSO) and Tu conditions. Four clusters are shown. (**c**) The Integrative Genome Viewer representation of intron retention in selected genes. (**d**) GO analysis of genes in four clusters showing enriched KEGG pathways. Data: box and whiskers with minimum to maximum. Statistical tests used: unpaired one-tailed Student's t-test for b.

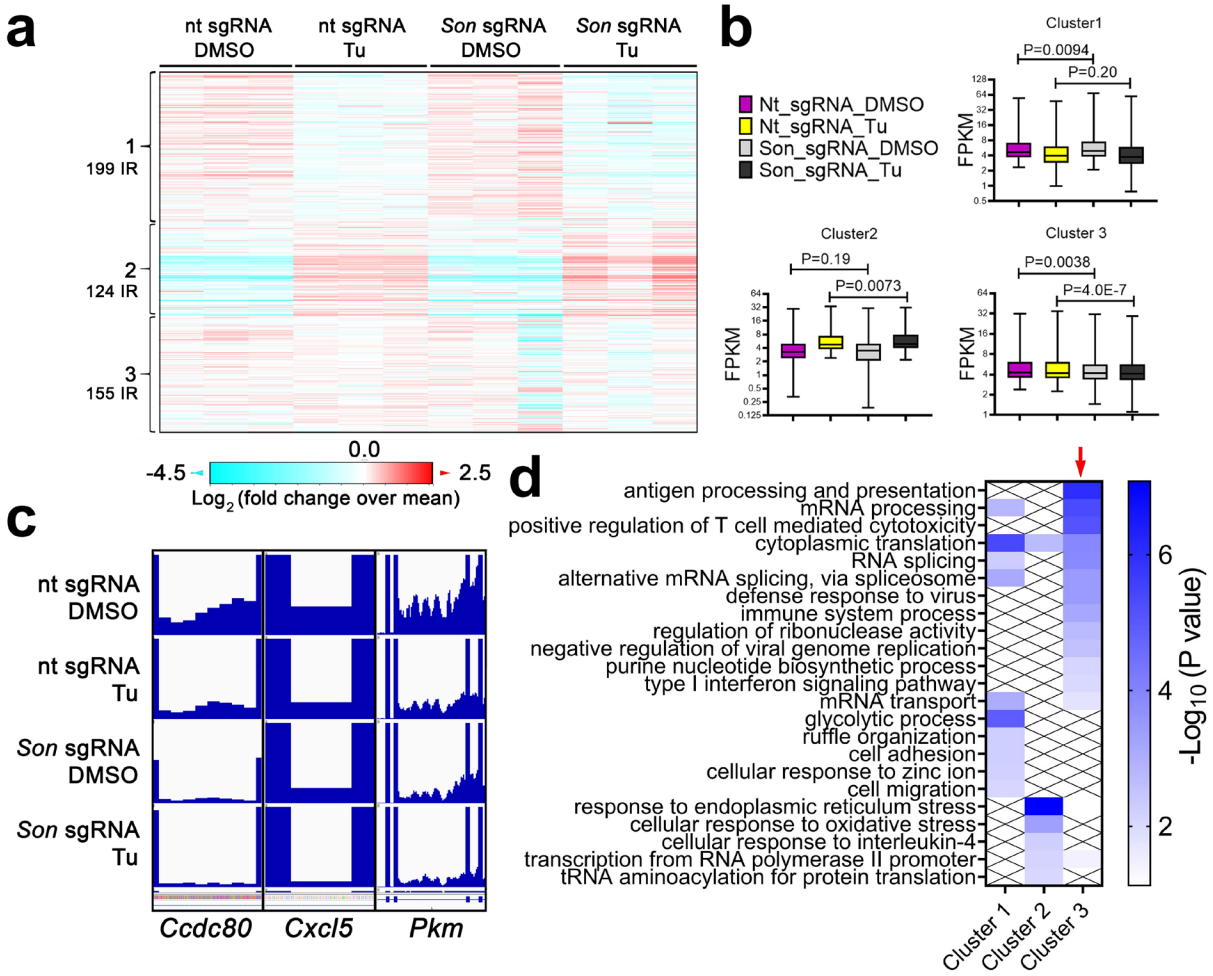

Supplementary Figure 6. SON overexpression decreases intron retention of protein processing and mRNA metabolism genes. Heat map (**a**) and quantification (**b**) of intron retention events in MEFs with control or SON overexpression under basal (DMSO) and Tu conditions. Three clusters are shown. (**c**) The Integrative Genome Viewer representation of intron retention in selected genes. (**d**) GO analysis of genes in three clusters showing enriched KEGG pathways. Data: box and whiskers with minimum to maximum. Statistical tests used: unpaired one-tailed Student's t-test for b.

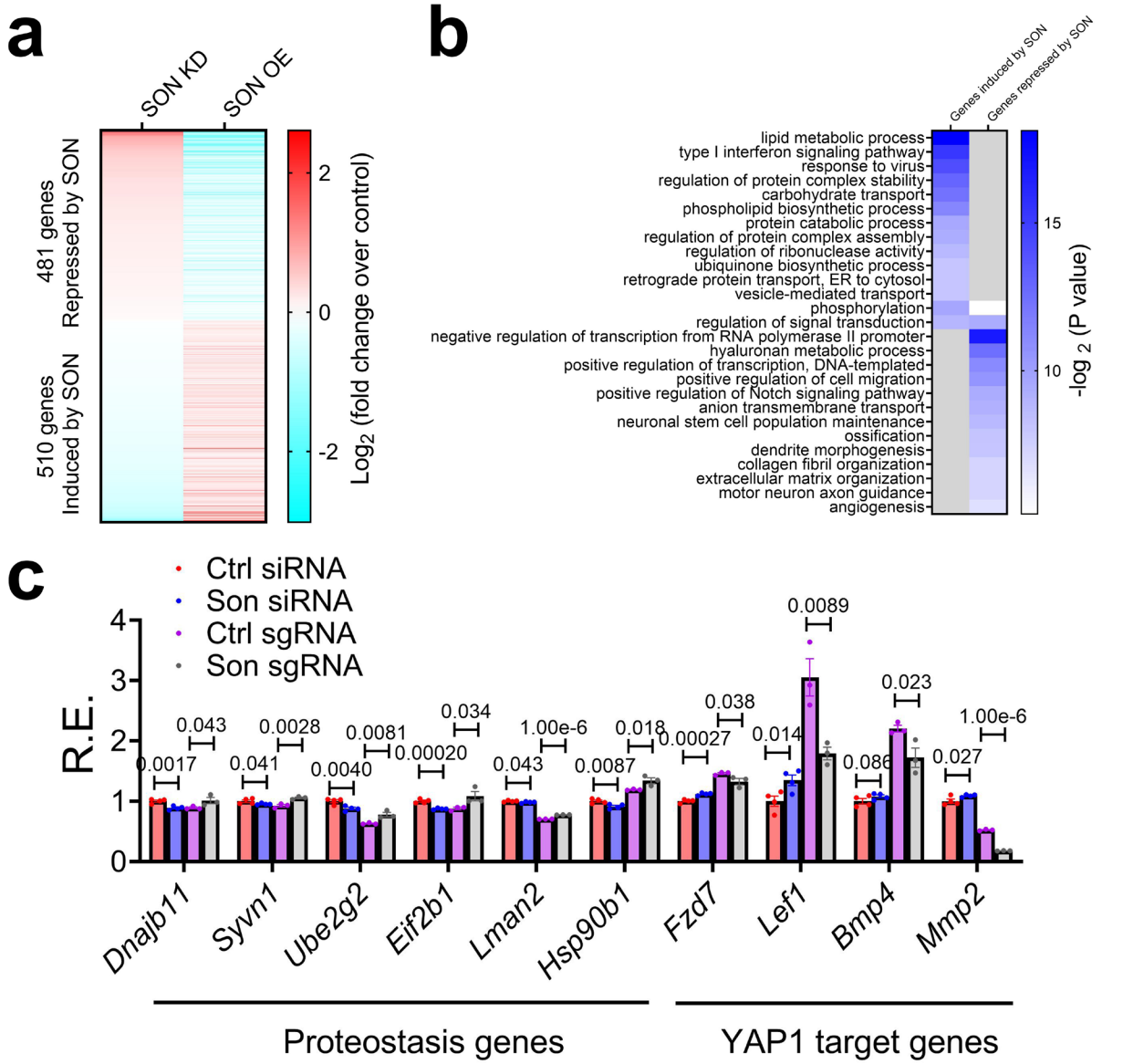

Supplementary Figure 7. SON reprograms opposing proteostasis and YAP1 transcriptional output under basal conditions. (**a**) Heat map of fold change of mature mRNA level in *Son* OE/KD MEFs compared to control MEFs under vehicle (DMSO) condition. All mature mRNAs in this heatmap are statistically differentially expressed (P<0.05) in both SON OE/KD conditions, compared to their respective controls. (**b**) GO analysis of these 481 and 501 genes. (**c**) Representative mature mRNA expression of proteostasis and YAP1 target genes (n=4 for Ctrl and *Son* siRNA and n=3 for Ctrl and *Son* sgRNA). Data: Mean ± S.E.M. Statistical tests used: unpaired one-tailed Student's t-test for c.

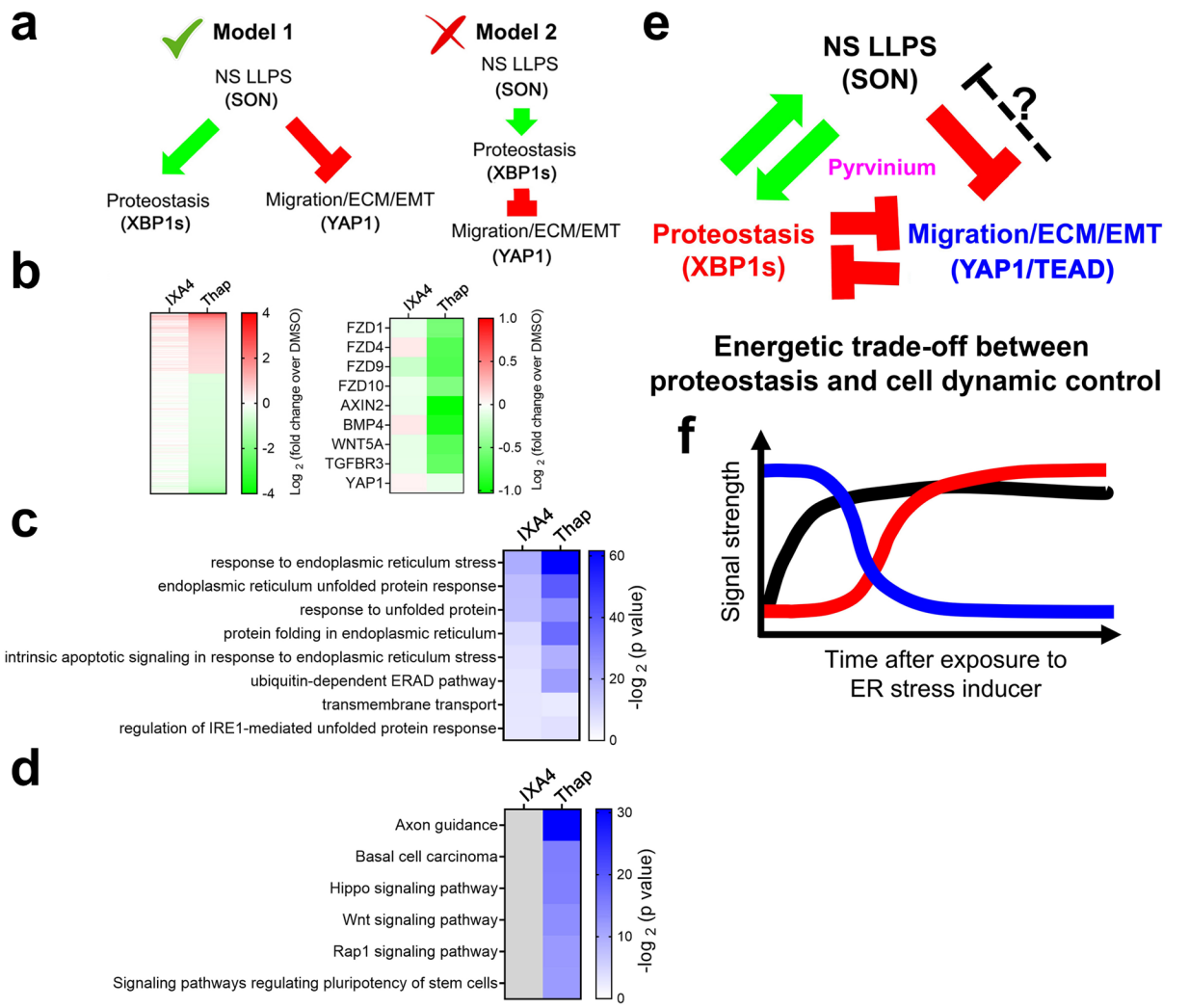

Supplementary Figure 8. Nuclear speckle LLPS dictates opposing proteostasis and YAP1 signaling. (**a**) Two models explaining the relationship among nuclear speckles LLPS dynamics, proteostasis and YAP1 transcriptional output. Our results support model 1. (**b**) Heatmap demonstrates relative fold change of gene expression relative to DMSO control in IXA4, or Thap treated HEK293T cells. All genes induced or repressed by at least 1.41-fold with p value smaller than 0.05 in Thap condition (left), and representative YAP1-related genes (right). (**c, d**) GO analysis of all upregulated (**c**) or downregulated (**d**) genes in either IXA4 or Thap treatment by at least 1.41-fold with a p-value smaller than 0.05. (**e**) An expanded model of how the LLPS of nuclear speckles can dictate proteostasis and YAP1 transcriptional output. Please see the main text for details. (**f, g**) Diagram showing temporal changes of NS' LLPS (black), proteostasis (red) and YAP1 transcriptional output (blue) signal during ER stress (**f**).

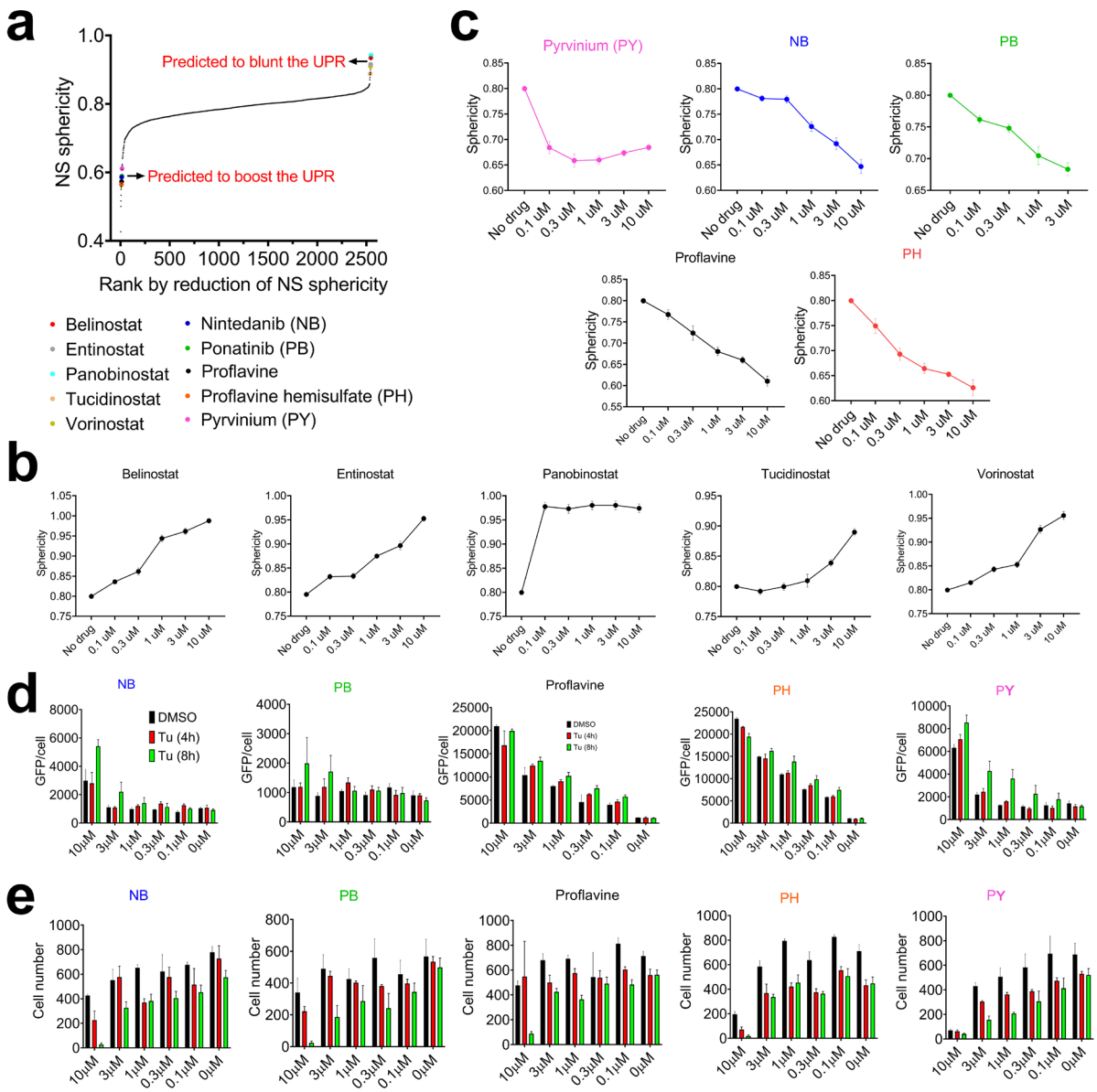

Supplementary Figure 9. HTS identifies compounds that alter nuclear speckle morphology and the UPR. (**a**) Compounds in the FDA-approved library ranked from lowest to highest on their ability to reduce NS sphericity. (**b**) Five drugs are shown to have a dose-dependent effect on increasing sphericity of NS (n=16). (**c**) Dose-dependent effects of drugs on decreasing NS sphericity (n=16). (**d, e**) GFP/cell (**d**) or cell number (**e**) measured in *Perk* promoter-driven dGFP reporter MEFs in the presence of Tu for four or eight hours after pre-treatment of different concentrations of drugs or DMSO for 24 hours (n=4). Data: Mean ± S.E.M.

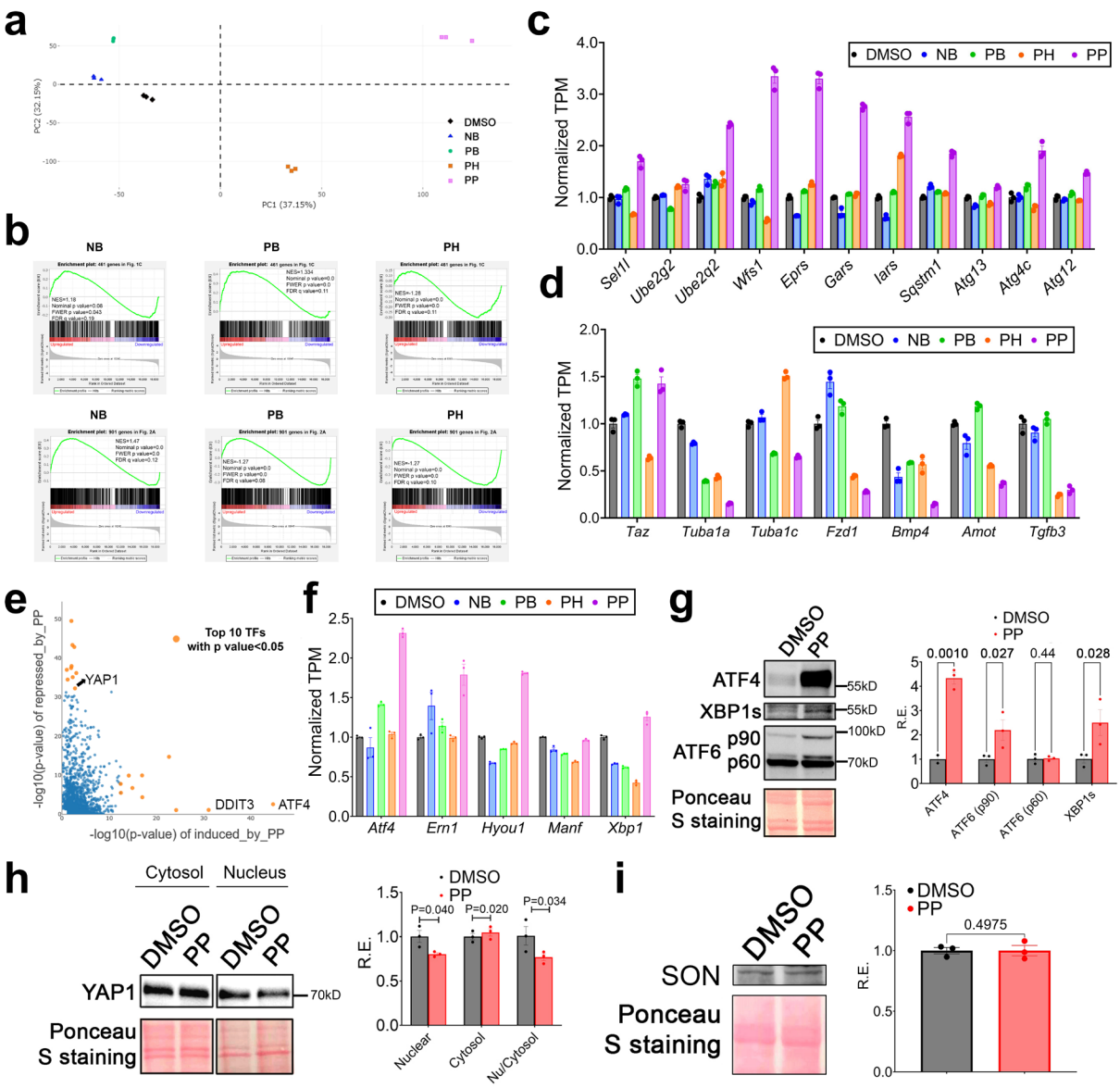

Supplementary Figure 10. PP is a bona fide nuclear speckle rejuvenator. (**a**) MEFs were treated with 3 μM NB, 1 μM PB, 3 μM PH, and 1 μM PP for 24 hours and RNA-seq was performed. PCA of global transcriptional response to drug treatments. (**b**) For each of the GSEA analysis, genes further activated by SON OE or further repressed by SON OE are compared to the transcriptome signatures of MEFs under different drug treatments. (**c, d**) Gene expression of select protein quality control (**c**) and YAP1 target genes (**d**) genes determined through mRNA-Seq (n=3). (**e**) LISA analysis listing log transformed p values for top predicted transcription regulators for genes upregulated (x-axis) and downregulated (y-axis) by PP. (**f**) Gene expression of select UPR genes determined through mRNA-Seq under different drugs treatment (n=3). (**g-i**) Western blot and quantification of UPR TFs (**g**), YAP1 nuclear and cytosol (**h**) and SON (**i**) level in response to 1 μM PP for 24 hours (n=3). Data: Mean ± S.E.M. Statistical tests used: unpaired one-tailed Student's t-test for g-i.

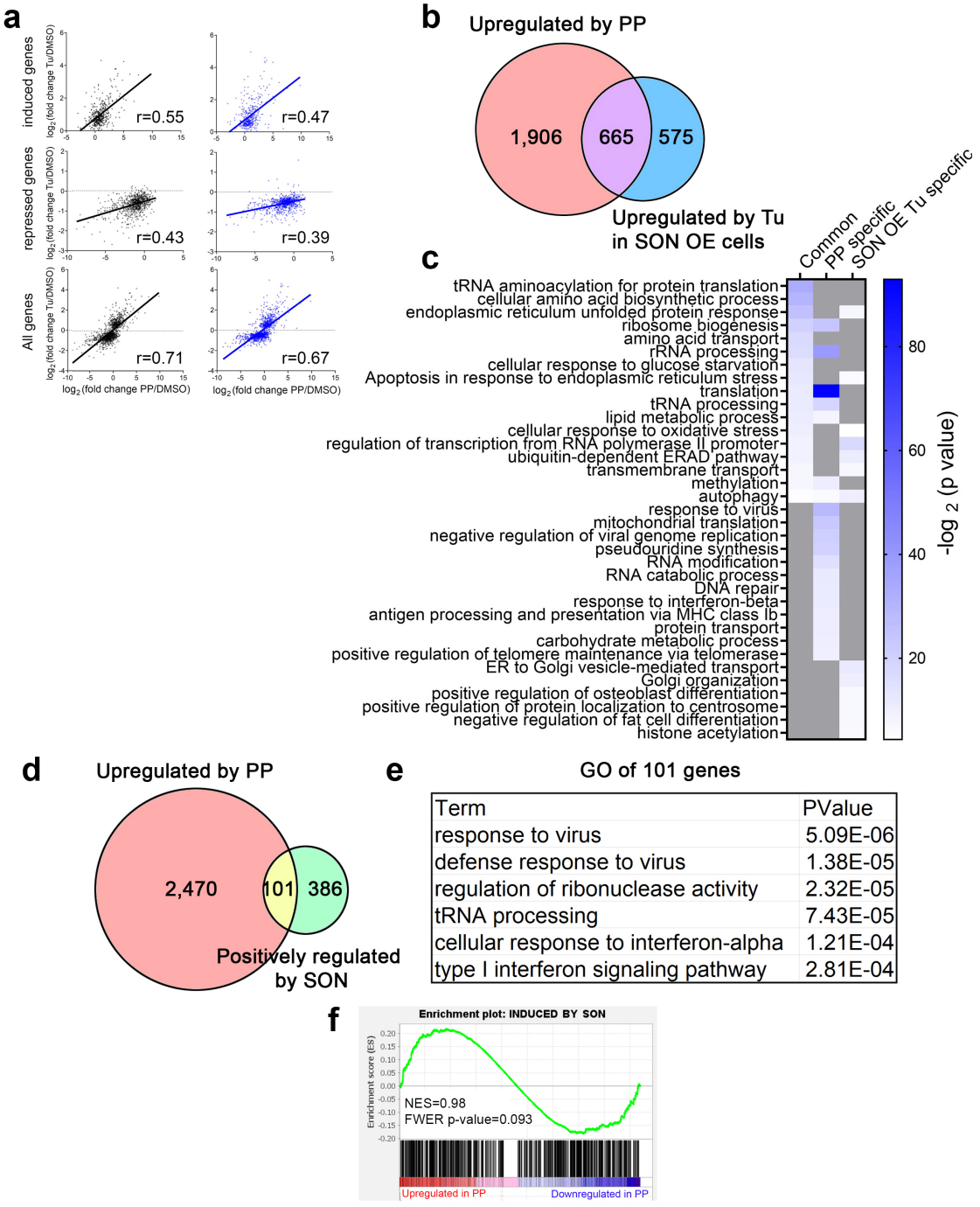

Term	PValue
response to virus	5.09E-06
defense response to virus	1.38E-05
regulation of ribonuclease activity	2.32E-05
tRNA processing	7.43E-05
cellular response to interferon-alpha	1.21E-04
type I interferon signaling pathway	2.81E-04

Supplementary Figure 11. Comparison of upregulated genes by PP and SON OE. (**a**) Scatter plot comparing the fold change of gene expression by PP (x-axis) and by Tu (y-axis) under SON OE or SON KD condition. Correlation coefficient and p value are shown for each plot. Chow test indicates statistically significant coefficients between the two linear regressions with p=0.00195. (**b, c**) Venn diagram showing (**b**) and GO analysis of (**c**) specific and commonly upregulated genes by PP and Tu in SON OE MEFs. (**d**) Venn diagram showing specific and common upregulated genes by PP and SON in MEFs. (**e**) GO analysis of common 101 genes. (**f**) GSEA analysis comparing genes upregulated by SON with those regulated by PP.

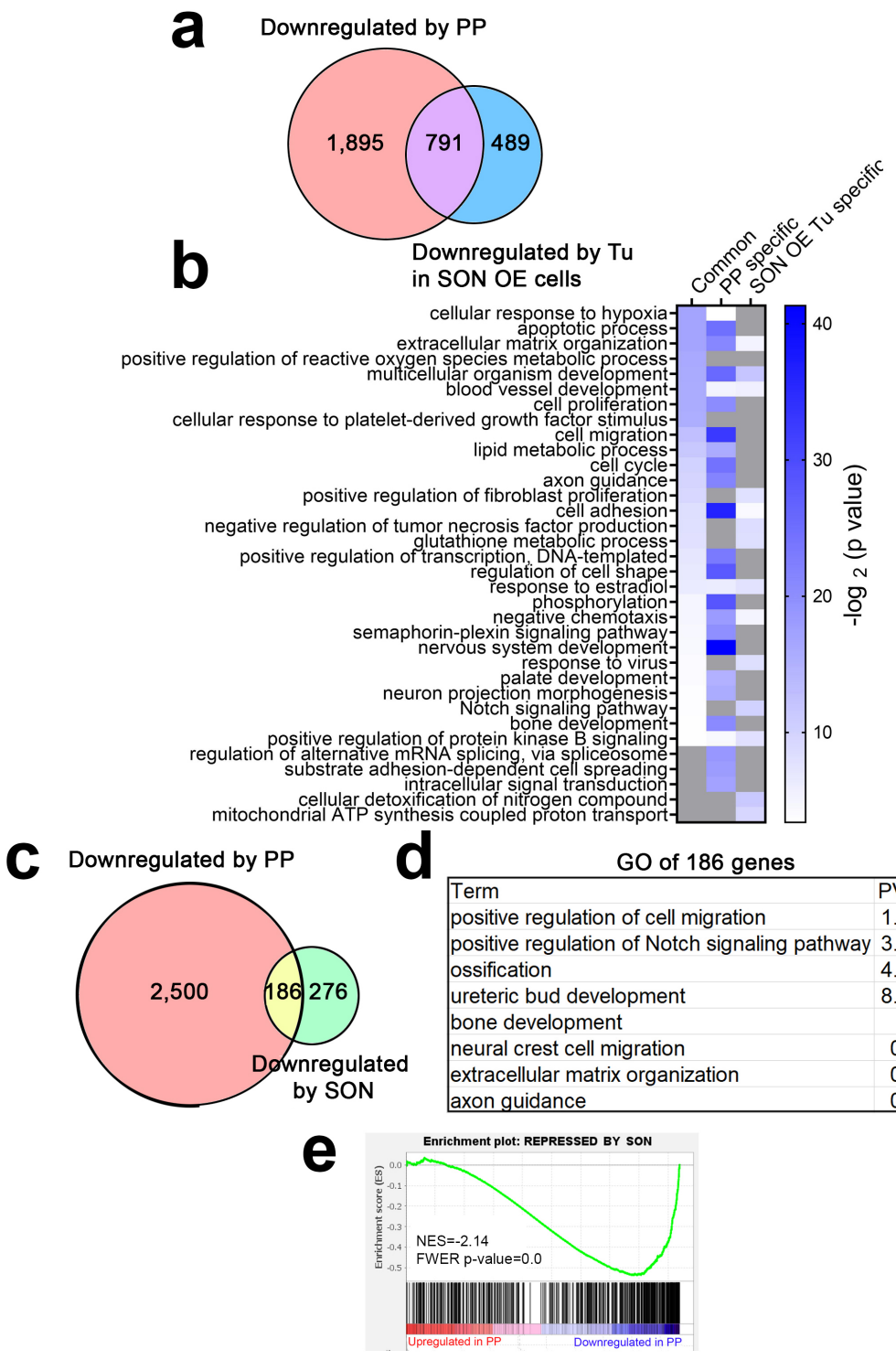

Term	PValue
positive regulation of cell migration	1.07E-04
positive regulation of Notch signaling pathway	3.71E-04
ossification	4.45E-04
ureteric bud development	8.10E-04
bone development	0.001
neural crest cell migration	0.00101
extracellular matrix organization	0.00108
axon guidance	0.00127

Supplementary Figure 12. Comparison of downregulated genes by PP and SON OE. (**a-b**) Venn diagram showing (**a**) and GO analysis of (**b**) specific and common downregulated genes by PP and Tu in SON OE MEFs. (**c**) Venn diagram showing specific and common downregulated genes by PP and SON in MEFs. (**d**) GO analysis of 186 common genes. (**e**) GSEA analysis comparing genes downregulated by SON with those regulated by PP.

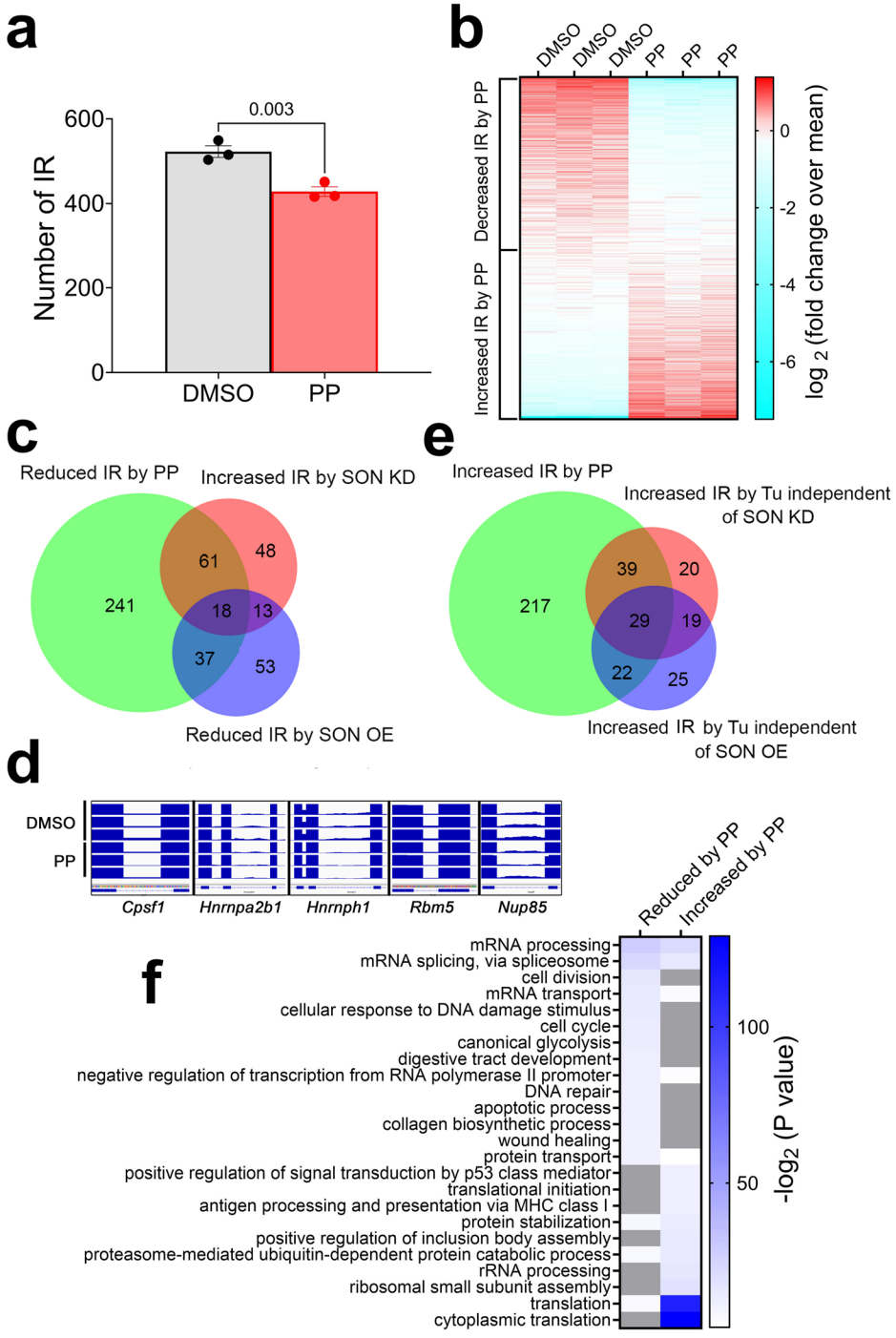

Supplementary Figure 13. Comparison of intron retention (IR) events among PP, SON OE and SON KD. (**a**) Quantification of IR under DMSO and PP condition (n=3). (**b**) Heatmap showing RPKM normalized level of retained introns in DMSO and PP condition. (**c, d**) Venn diagram comparing genes with specific or common IRs between different conditions. (**e**) Genome browser view of selective genes with reduced IR by PP. (**f**) GO analysis of genes with increased or reduced IR by PP. Data: Mean ± S.E.M. Statistical tests used: unpaired one-tailed Student's t-test for a.

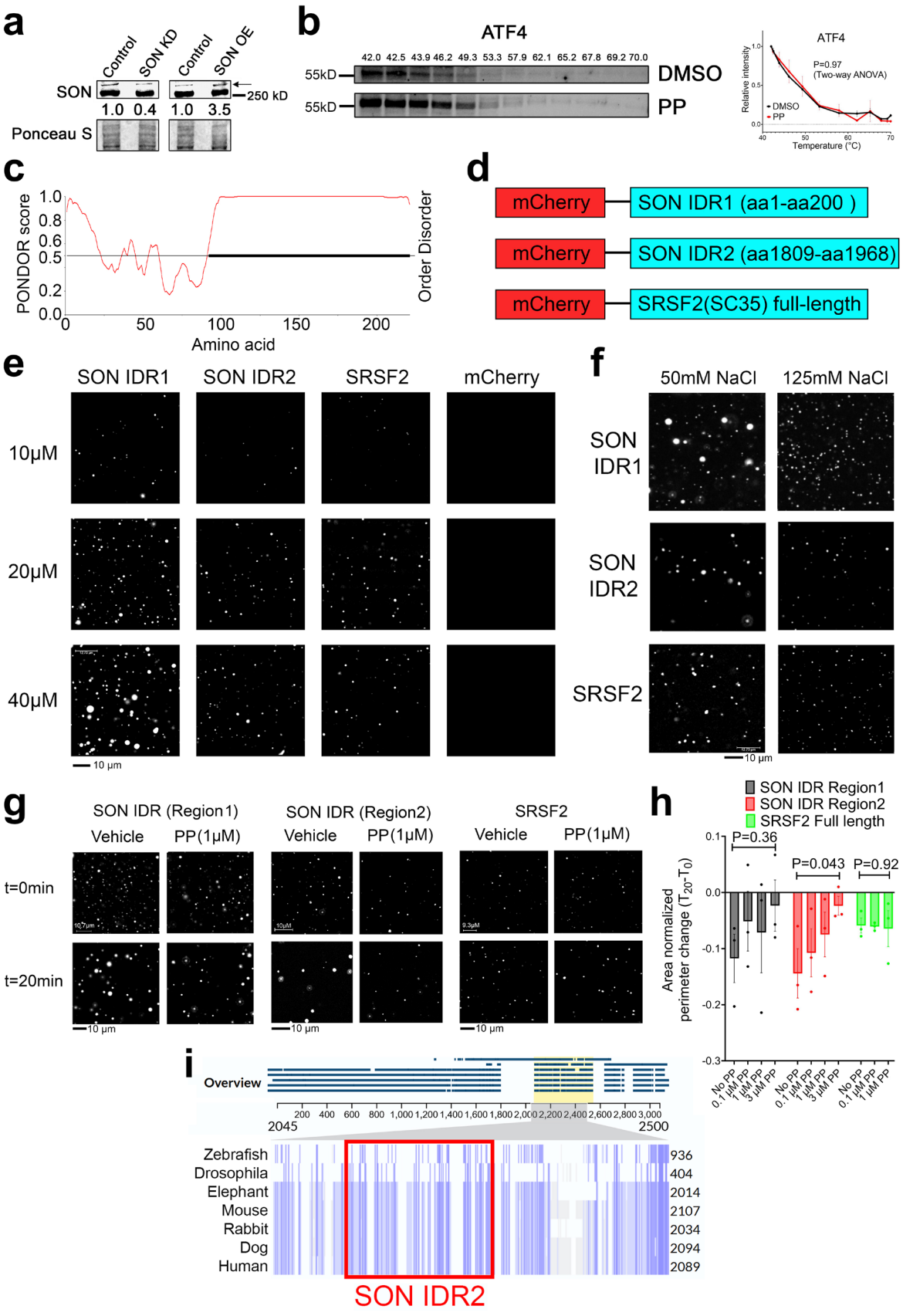

Supplementary Figure 14. PP directly targets SON to modulate nuclear speckle LLPS dynamics. (**a**) Western blots of SON with siRNA-mediated knockdown and SON OE. (**b**) CETSA of ATF4 with 3μM PP. Both representative blot and quantification from independent replicates are shown (n=2 for DMSO and n=3 for PP). (**c**) Computational prediction of IDR in mouse SRSF2 (SC35) protein. (**d**) Diagram illustrating the constructs for droplet formation assay (**e**) Representative images of droplet formation assay with different concentrations of recombinant protein at 125mM NaCl. (**f**) Representative images of droplet formation assay with different salt concentrations with 20μM recombinant proteins. (**g, h**) Representative images of droplet formation assay with different recombinant proteins (**g**) and quantification (**h**) of area-normalized perimeter changes in the time span of 20 minutes with 50mM NaCl (n=3). (**i**) Alignment of protein sequences of SON orthologs in seven different species. SON IDR2 is located within the most conserved region (highlighted by light yellow). Data: Mean ± S.E.M. Statistical tests used: Two-way ANOVA for b and one-way ANOVA for h.

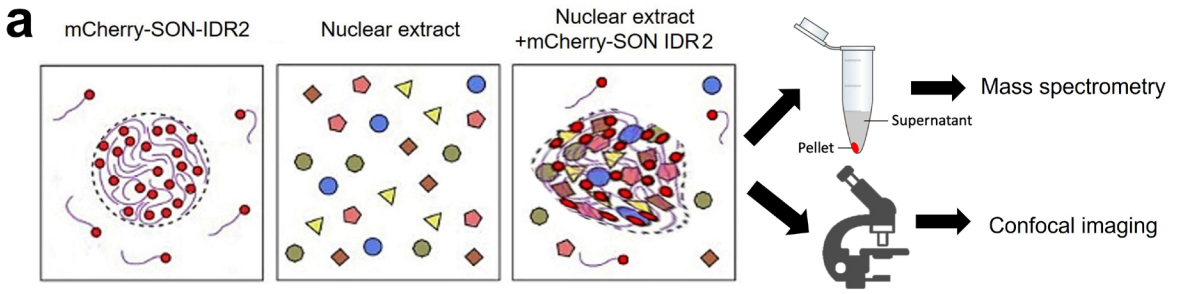

b

Gene name	Description	Log 2(fold enrichment over input)	p value	Identified in Saitoh et al	Identified in Dopie et al
SRSF1	Serine/arginine-rich splicing factor 1	6.29	0.0008	Yes	Yes
FUS	RNA-binding protein FUS	5.44	0.0150	Yes	Yes
ANXA7	Annexin A7	4.34	0.0081	No	No
AHNK	Neuroblast differentiation-associated protein	4.31	0.0390	No	Yes
SRSF2	Serine/arginine-rich splicing factor 2	4.08	0.0103	Yes	Yes
PDIP3	Polymerase delta-interacting protein 3	3.95	0.0048	No	Yes
HNRPC	Isoform C1 of Heterogeneous nuclear ribonucleoproteins C1/C2	3.80	0.0212	Yes	No
RPS14	40S ribosomal protein S14	3.71	0.0007	No	No
SRSF3	Serine/arginine-rich splicing factor 3	3.66	0.0189	Yes	Yes
ZN638	Zinc finger protein 638	3.61	0.0440	No	No
ANX11	Annexin A11	3.17	0.0475	No	Yes
RBMX2	RNA-binding motif protein, X-linked 2	3.16	0.0147	Yes	No
ROA0	Heterogeneous nuclear ribonucleoprotein A0	3.01	0.0082	Yes	No
SRSF10	Serine/arginine-rich splicing factor 10	2.95	0.0037	Yes	Yes
EWSR1	RNA-binding protein EWS	2.91	0.0171	Yes	Yes

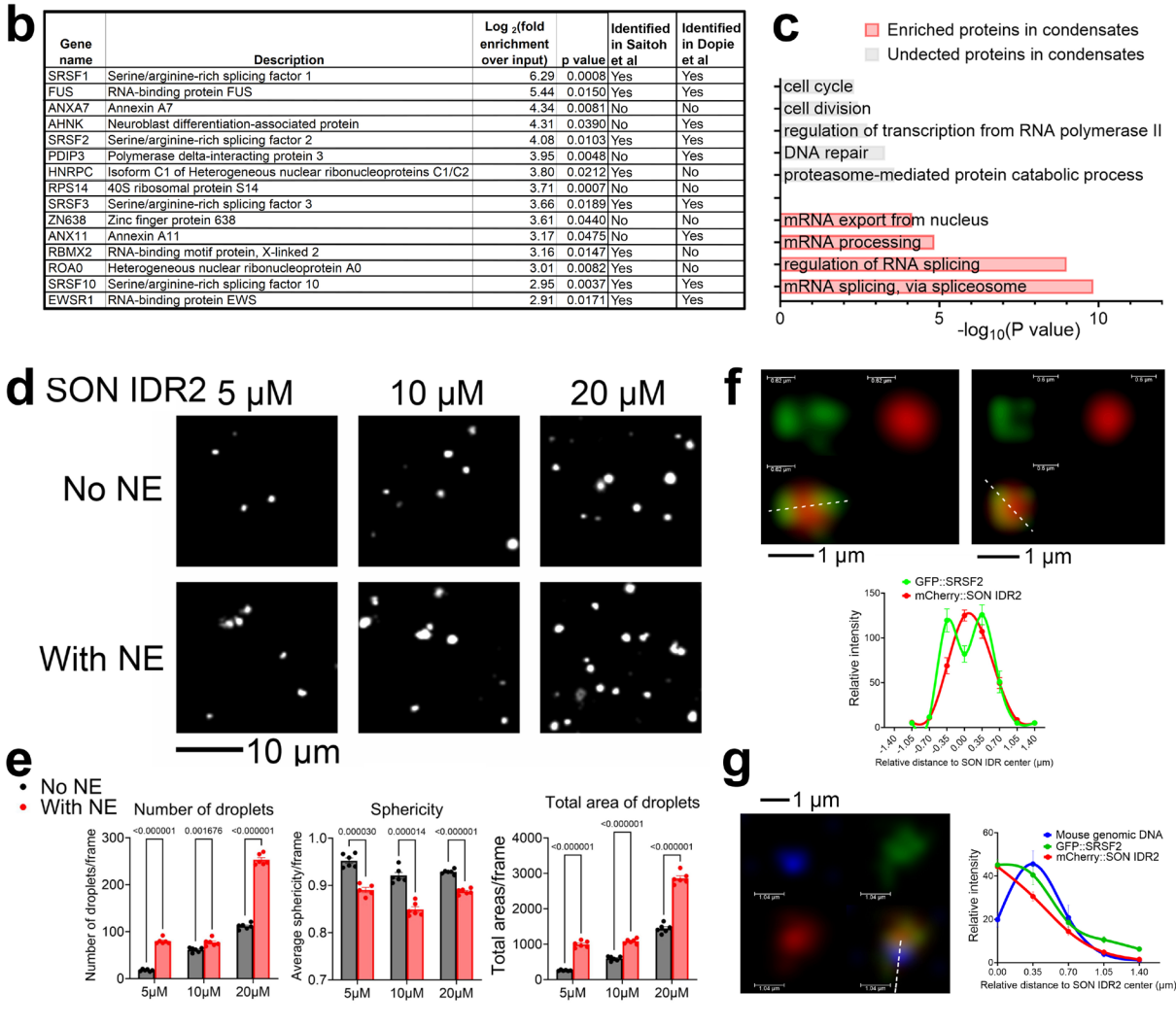

Supplementary Figure 15. PP modulates nuclear speckle LLPS dynamics in a cell-free system. (**a**) Diagram showing NE-supplemented SON IDR2 condensates are expected to compartmentalize splicing factors and exhibit less spherical morphology. (**b**) NE-supplemented SON IDR2 condensates are spun down and subject to mass spectrometry. Top 15 proteins mostly enriched in SON IDR2-compartmentzlied condensates with p value<0.05, and the status of whether these proteins have been identified in nuclear speckles in cells in two datasets [52, 53] (**c**) GO of top enriched biological pathways of proteins depleted or enriched in SON IDR2-compartmentzlied condensates. (**d, e**) Representative images of droplet formation assay with

increasing concentration of SON IDR2 with or without NE supplementation (**e**) and quantification (**e**) of the number, sphericity and total areas of droplets (n=6). (**f**) Representative images and quantification of spatial distribution of mCherry::SON IDR2 and GFP::SRSF2. (**g**) Representative images and quantification of spatial distribution of mCherry::SON IDR2, GFP::SRSF2 and mouse genomic DNA. Data: Mean ± S.E.M. Statistical tests used: unpaired one-tailed Student's t-test for e.

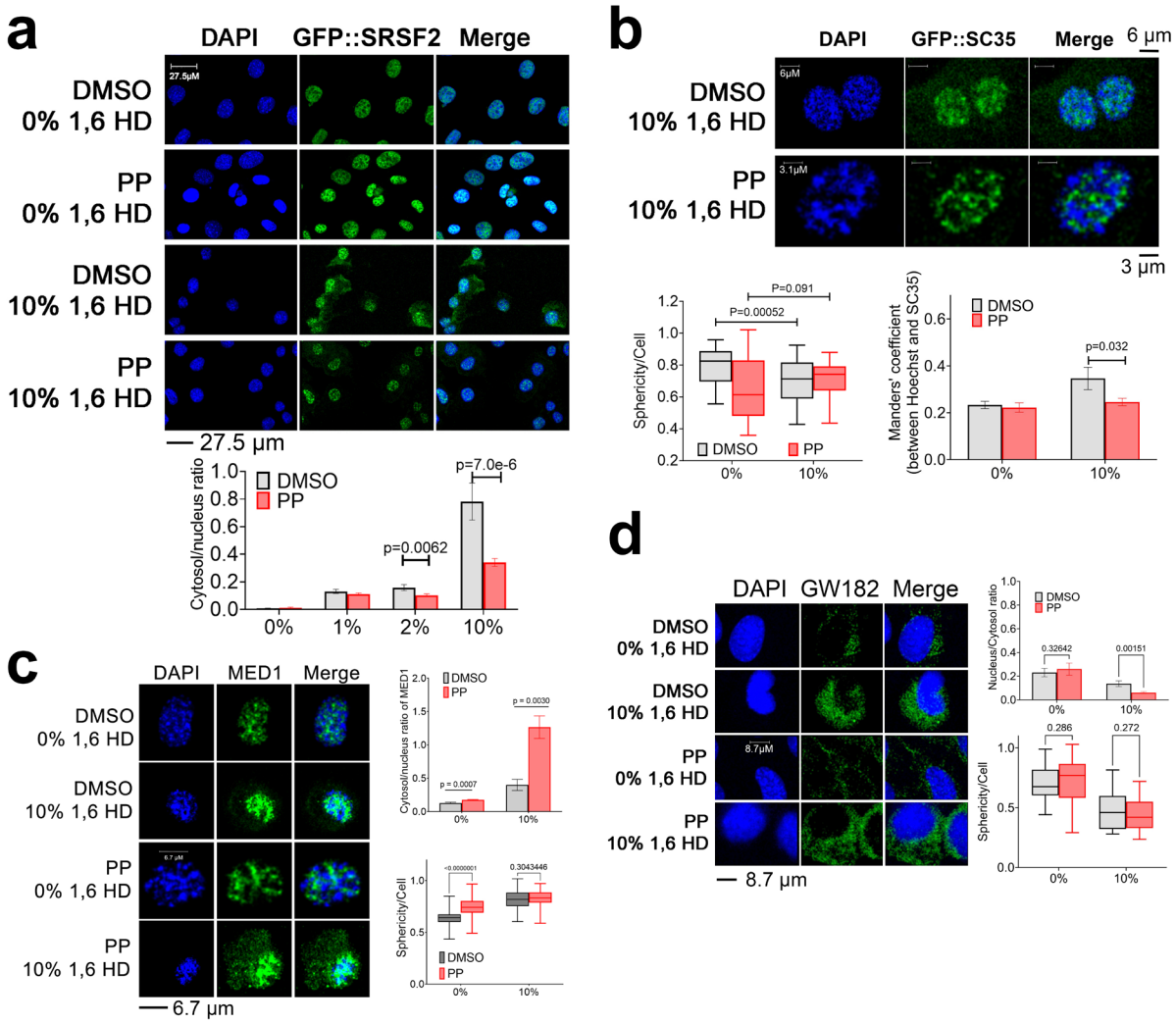

Supplementary Figure 16. PP alters the sensitivity of different condensates to 1,6 hexanediol. (**a**) 1,6 hexanediol sensitivity assay with representative images and quantification (n=20~95) of the ratio of cytosol over nuclear intensity of GFP::SRSF2 signal. (**b**) 1,6 hexanediol sensitivity assay with representative images and quantification of sphericity (n=24~50) of GFP::SRSF2 signal and Manders' coefficient (n=10~14) of signals of GFP and Hoechst. (**c**) 1,6 hexanediol sensitivity assay with representative images and quantification of ratio of cytosol to nuclear MED1 signal (n=19~29) and sphericity of MED1 signal (n=31~75). (**d**) 1,6 hexanediol sensitivity assay with representative images and quantification of ratio of cytosol to nuclear GW182 signal (n=16~54) and sphericity (n=19~97) of GW182 signal. Data: Mean ± S.E.M. Statistical tests used: unpaired one-tailed Student's t-test for all data.

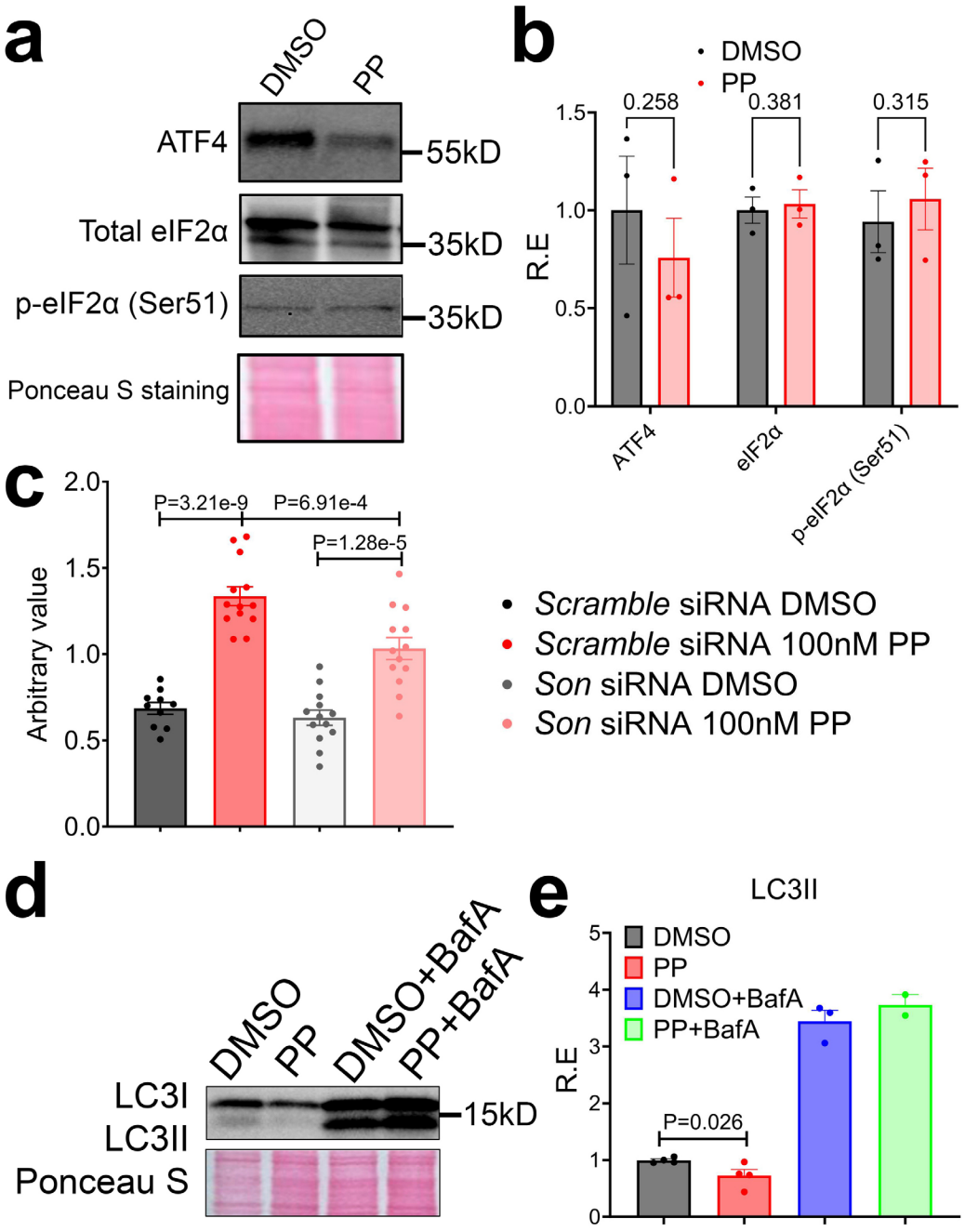

Supplementary Figure 17. Nanomolar concentration of PP promotes UPS and ALP without inducing cellular stress. (**a, b**) MEFs were treated with DMSO or 100nM PP for 24 hours. Representative western blot (**a**) and quantification (**b**) of different proteins (n=3). (**c**) MEFs were transiently transfected with scrambled or Son siRNA for 24 hours before treated with DMSO or 100nM PP for another 24 hours. 20S proteasome activity assay was then performed (n=10~13). (**d, e**) MEFs were treated with vehicle control or 1μM PP for ~22 hours and then co-treated with or without Baf A (100nM for 22 hours) (n=2~4). Representative western blot image (**d**) and quantification (**e**) of LC3II and LC3II/LC3I ratio. Data: Mean ± S.E.M. Statistical tests used: unpaired one-tailed Student's t-test for all data.

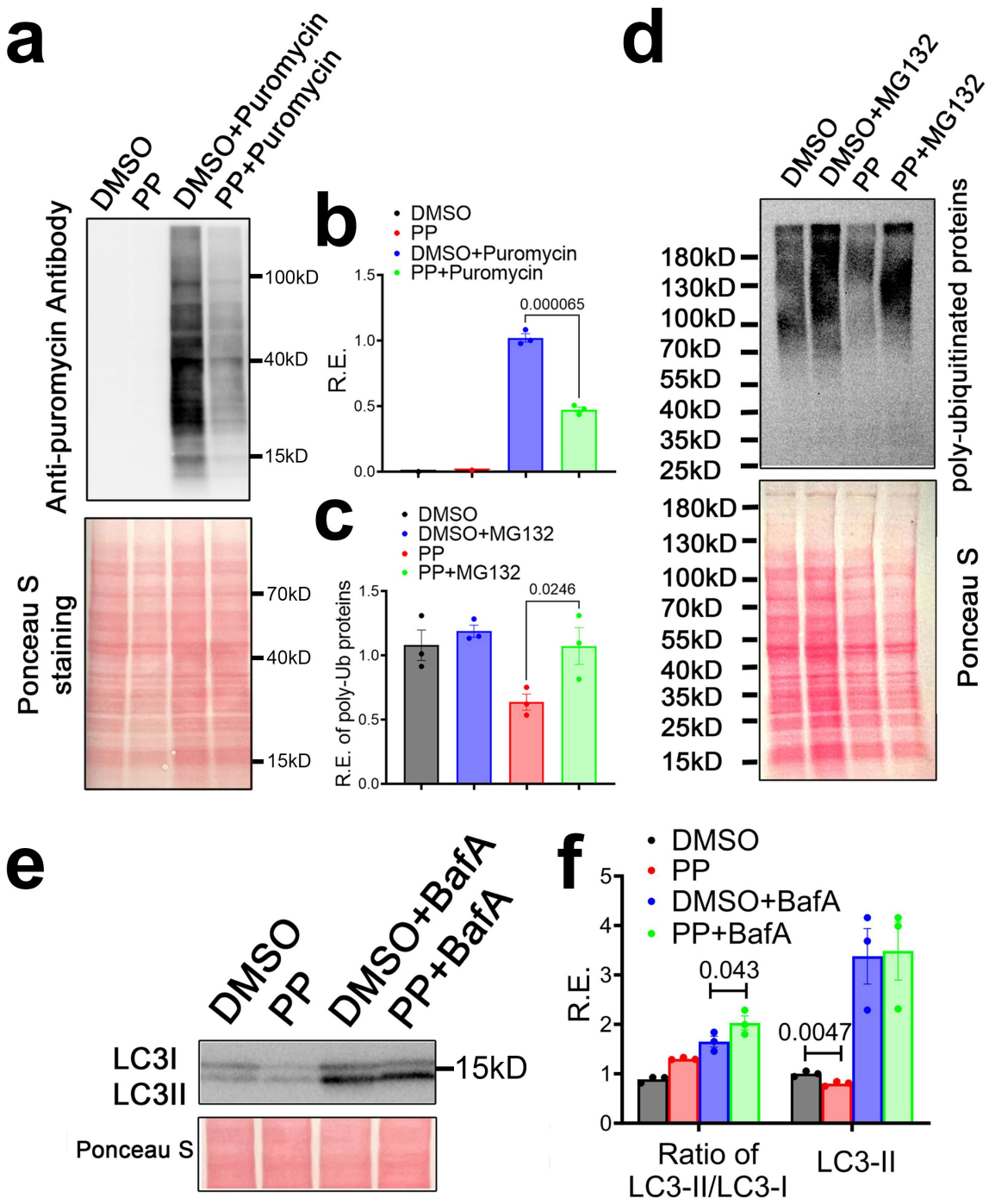

Supplementary Figure 18. Micromolar PP promotes autophagy and UPS activity and represses translation. MEFs were treated with vehicle control or 1μM PP for ~24 hours (22 hours for **e** and **f**) and then co-treated with or without puromycin (10 μg/mL for 30 minutes), MG132 (10μM for 110 minutes) or Baf A (100nM for 22 hours) (n=3 for all samples). Western blot and quantification of puromycin-incorporated proteins (**a, b**), poly-ubiquitinated protein (**c, d**) and LC3II and LC3II/LC3I ratio (**e, f**). Data: Mean ± S.E.M. Statistical tests used: unpaired one-tailed Student's t-test for all data.

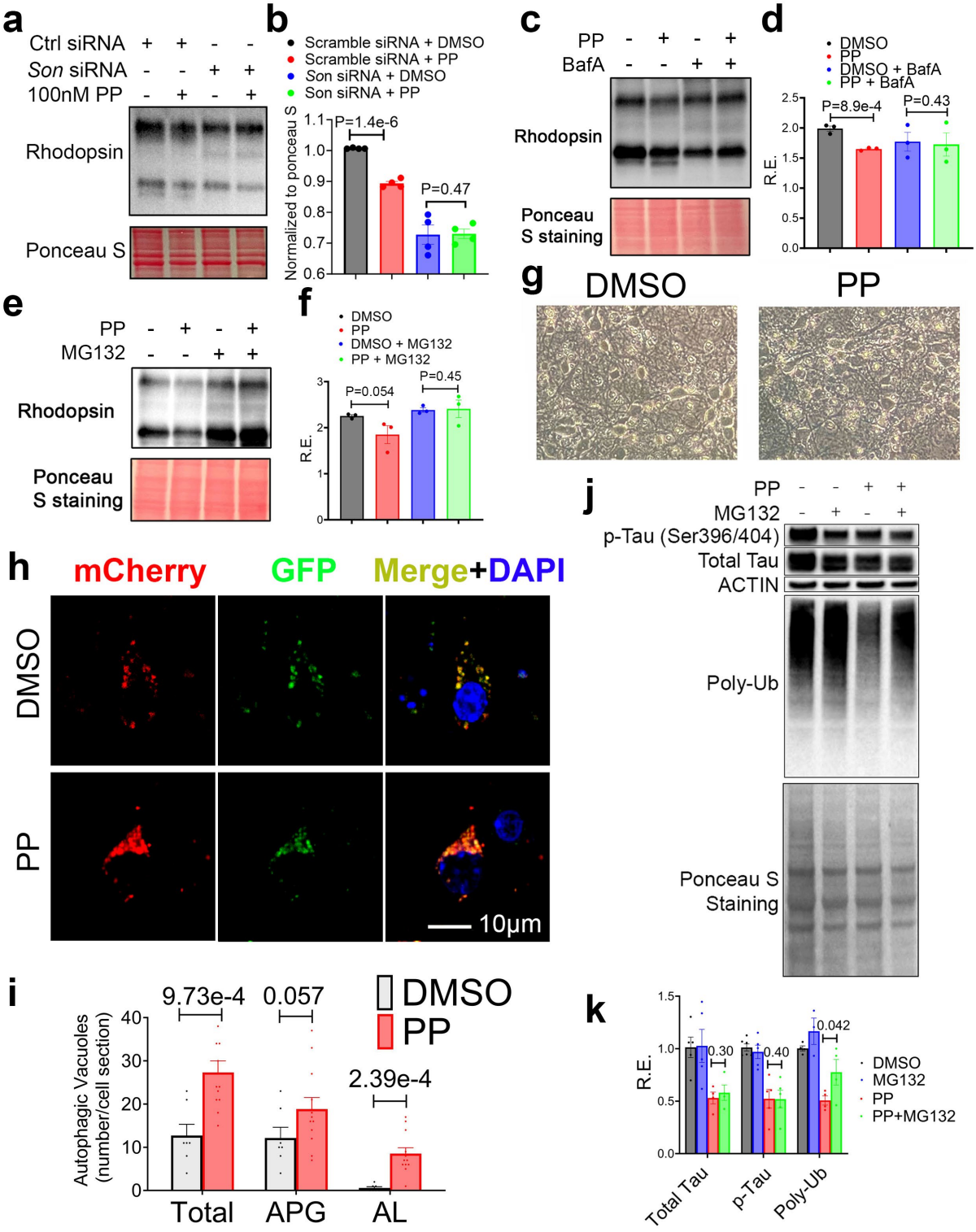

Supplementary Figure 19. Pyrvinium pamoate reduces pathological Tau and Rhodopsin level by boosting autophagy and UPS activity. (**a, b**) NIH3T3 RHO^{P23H} cells were transfected with scrambled or *Son* siRNA for 24 hours before treated with DMSO or 0.1μM PP for another 24 hours. Western blot (**a**) and quantification (**b**) of RHO^{P23H} level (n=4). (**c, d**) NIH3T3 RHO^{P23H} cells

were treated with 0.1μM PP and co-treated with or without BafA (100nM) for 24 hours. Western blot (**c**) and quantification (**d**) of RHO^{P23H} level (n=3). (**e, f**) NIH3T3 RHO^{P23H} cells were co-treated with or without MG132 (10μM for 120 minutes). Western blot (**e**) and quantification (**f**) of RHO^{P23H} level (n=3). (**g**) Representative images of primary mouse neurons treated with DMSO or 0.5 μM PP for 24 hours. (**h, i**) Representative images showing an increase of the number of mCherry positive puncta in primary neurons cultured in the presence of 0.1μM PP for 12 hours, with zoomed in images of regions marked with white rectangles (**h**). Quantification of the number of total vacuoles, autophagosome and autolysosomes (n=7~12) (**i**). (**j, k**) Tau P301S-expressing primary neurons were co-treated with vehicle or 0.1μM PP in the presence or absence of MG132 (10μM) for 12 hours and western blot (**j**) and quantification (**k**) of different proteins (n=3~5). All data mean ± S.E.M. Statistical tests used: unpaired one-tailed Student's t-test for all data.

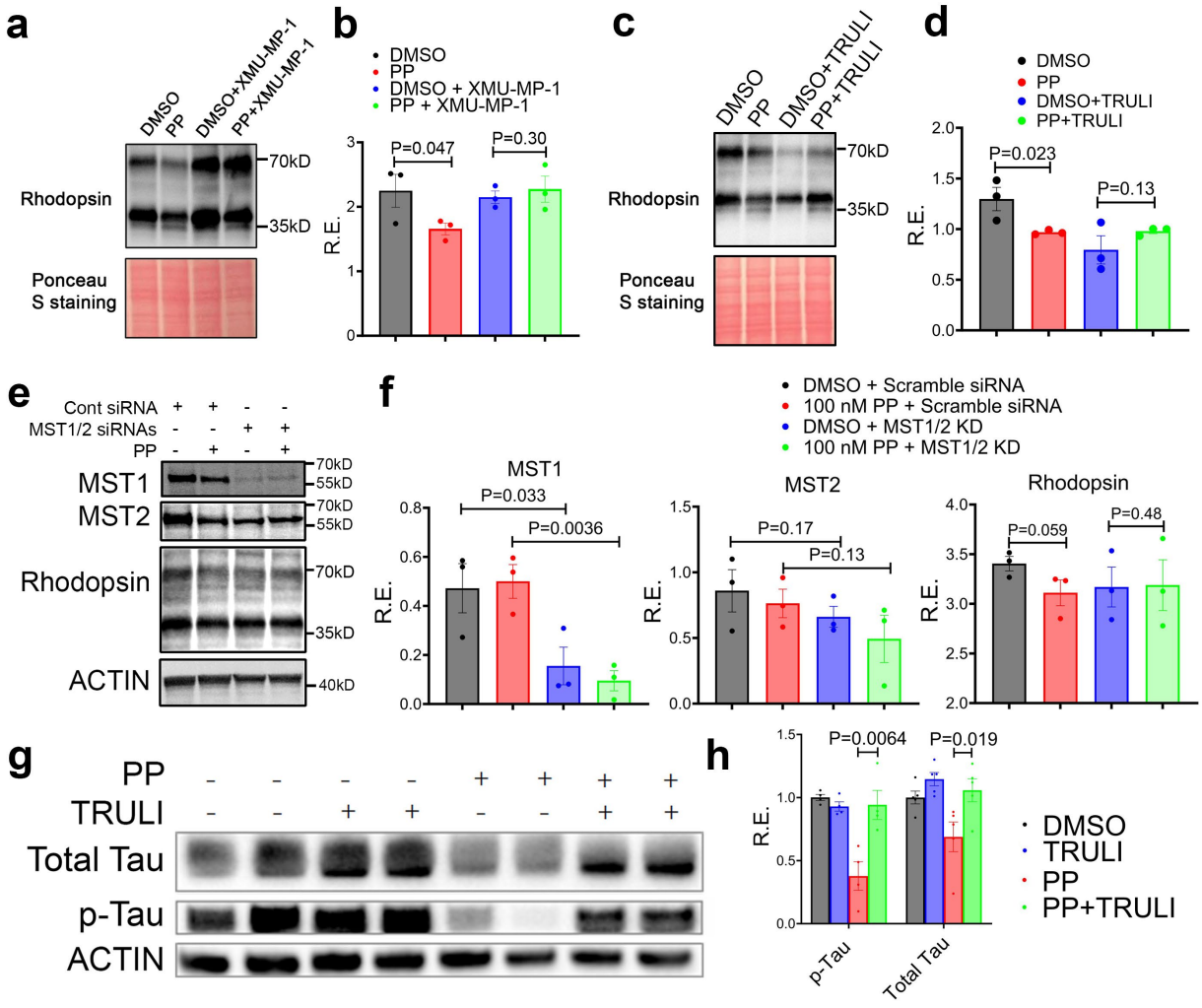

Supplementary Figure 20. Pyrvinium pamoate reduces pathological Rhodopsin level in a manner that depends on reduced YAP1 activity. (**a, b**) NIH3T3 RHO^{P23H} cells were treated with 0.1μM PP for 24 hours and co-treated with or without XMU-MP-1 (1μM). Western blot (**a**) and quantification (**b**) of RHO^{P23H} level (n=3). (**c, d**) NIH3T3 RHO^{P23H} cells were treated with 0.1μM PP for 24 hours and co-treated with or without TRULI (1μM). Western blot (**c**) and quantification (**d**) of RHO^{P23H} level (n=3). (**e, f**) NIH3T3 RHO^{P23H} cells were transiently transfected with scrambled or Mst1/Mst2 siRNAs for 24 hours and then treated with DMSO or 0.1μM PP for another 24 hours. Western blot (**e**) and quantification (**f**) of MST1/2 and RHO^{P23H} level (n=3). (**g, h**) Tau P301S-expressing primary neurons were co-treated with vehicle or 0.1μM PP in the presence or absence of YAP1 activator TRULI (10μM) for 12 hours and western blot (**g**) and quantification (**h**) of different proteins (n=4). All data: mean ± S.E.M. Statistical tests used: unpaired one-tailed Student's t-test for all data.

Genes upregulated by PP

ATG13

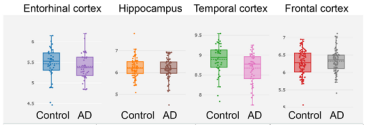

Brain region	Log 2 fold change	P- value	FDR
Entorhinal Cortex	-0.04	0.655	0.788
Hippocampus	-0.04	0.66	0.827
Temporal Cortex	-0.23	0.008	0.042
Frontal Cortex	0.09	0.056	0.154

EDEM1

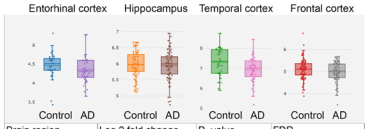

Brain region	Log 2 fold change	P- value	FDR
Entorhinal Cortex	-0.13	0.116	0.27
Hippocampus	-0.01	0.881	0.947
Temporal Cortex	-0.41	0.004	0.027
Frontal Cortex	-0.12	0.117	0.547

GARS

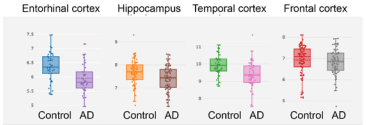

Brain region	Log 2 fold change	P- value	FDR
Entorhinal Cortex	-0.43	0.000428	0.01
Hippocampus	-0.26	0.006	0.061
Temporal Cortex	-0.5	0.001	0.008
Frontal Cortex	-0.1	0.169	0.319

HYOU1

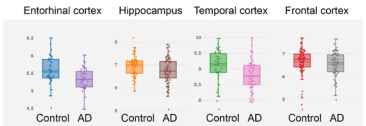

Brain region	Log 2 fold change	P- value	FDR
Entorhinal Cortex	-0.25	0.006	0.043
Hippocampus	-0.21	0.019	0.113
Temporal Cortex	-0.3	0.006	0.035
Frontal Cortex	-0.1	0.152	0.296

IARS

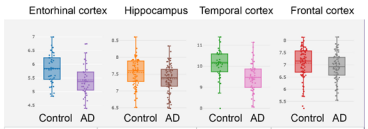

Brain region	Log 2 fold change	P- value	FDR
Entorhinal Cortex	-0.42	0.002	0.02
Hippocampus	-0.17	0.023	0.127
Temporal Cortex	-0.67	1.03E-05	0.000428
Frontal Cortex	-0.21	0.005	0.031

SEL1L

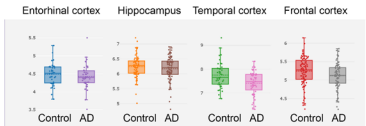

Brain region	Log 2 fold change	P- value	FDR
Entorhinal Cortex	-0.05	0.522	0.688
Hippocampus	-0.09	0.225	0.473
Temporal Cortex	-0.35	0.003	0.021
Frontal Cortex	-0.09	0.076	0.187

Genes downregulated by PP

AMOT

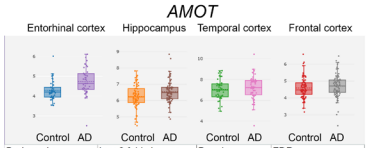

Brain region	Log 2 fold change	P- value	FDR
Entorhinal Cortex	0.44	0.002	0.022
Hippocampus	0.28	0.023	0.13
Temporal Cortex	0.15	0.522	0.721
Frontal Cortex	0.1	0.182	0.333

TEAD1

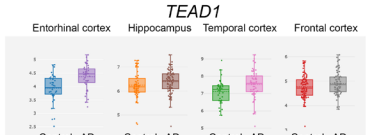

Brain region	Log 2 fold change	P- value	FDR
Entorhinal Cortex	0.41	0.001	0.012
Hippocampus	0.12	0.205	0.449
Temporal Cortex	0.42	0.009	0.047
Frontal Cortex	0.16	0.055	0.434

YAP1

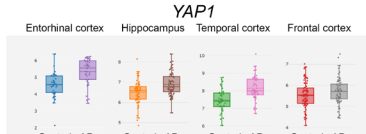

Brain region	Log 2 fold change	P- value	FDR
Entorhinal Cortex	0.69	6.01E-05	0.004
Hippocampus	0.37	0.00027	0.009
Temporal Cortex	0.7	3.180E-06	0.0002095
Frontal Cortex	0.18	0.026	0.093

Supplementary Figure 21. Gene signatures in human AD subjects are opposite from those regulated by PP revealed by bulk RNA-Seq. Relative gene expressions in different brain regions of human AD subjects normalized to control subjects as reported in [87].

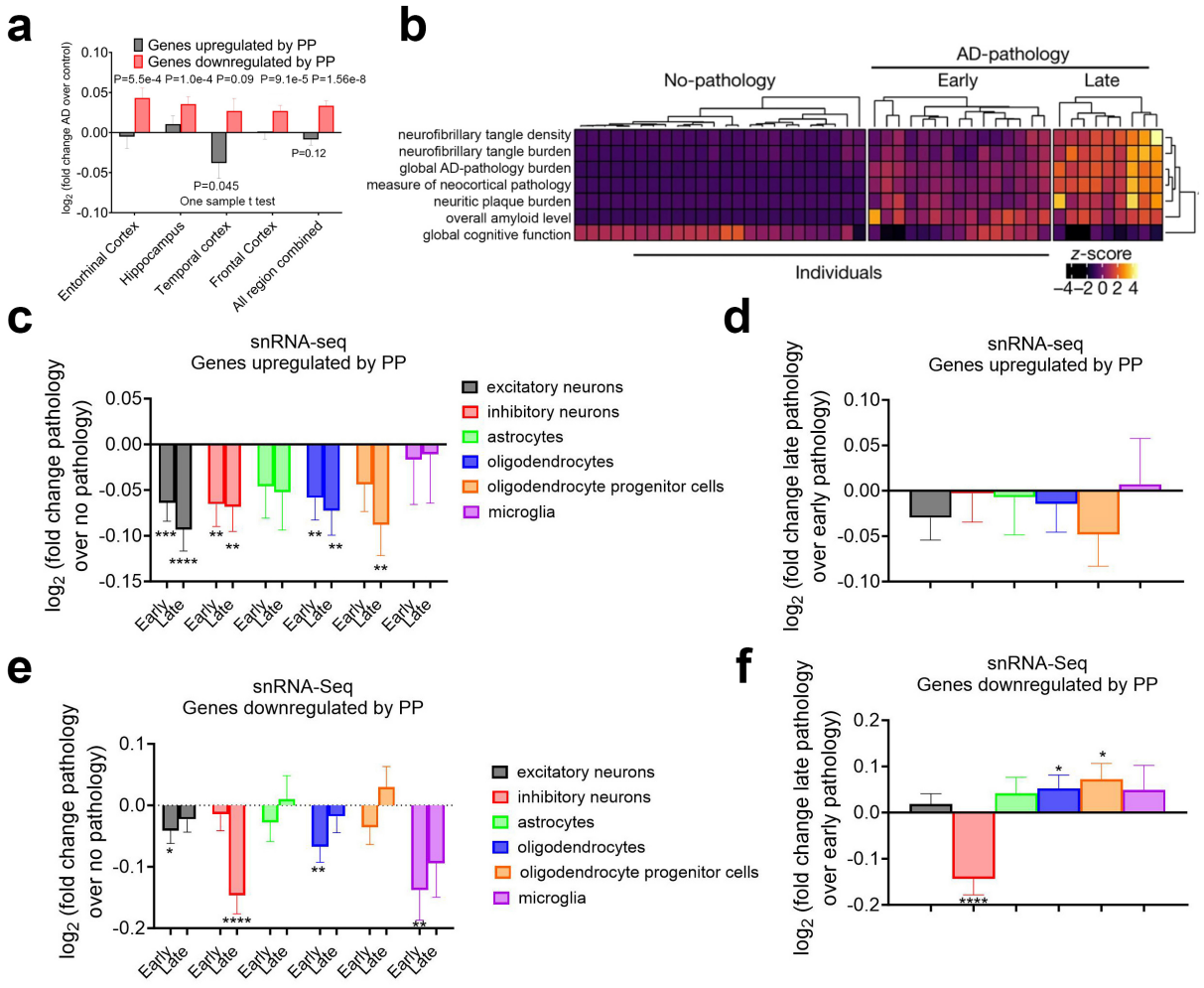

Supplementary Figure 22. Gene signatures in late-stage human AD subjects with severe tauopathy are opposite from those regulated by PP. (**a**) Log $_2$ transformed values of fold change of gene expression of different individual or combined brain regions of AD versus control human subjects for top genes that were either upregulated or downregulated by PP (with a $\log_2$ fold change > 1.5) in MEFs. (**b**) Phenotypic clustering of 48 individuals (columns) using seven clinicopathological variables as reported and adapted from [88]. (**c-f**) Log $_2$ transformed values of fold change of mean gene expression of different cell types of early or late AD versus no pathology human subjects for top genes that were either upregulated (**c**) or downregulated by PP in MEFs (**e**). Log 2 transformed values of fold change of mean gene expression of different cell types of late AD versus early AD human subjects for top genes that were either upregulated (**d**) or downregulated by PP in MEFs (**f**). Data: Mean ± S.E.M. Statistical tests used: unpaired one-tailed Student's t-test for a. One sample t-test (one-tailed). * p<0.05, ** p<0.01, *** p<0.001, **** p<0.0001 for c-f.

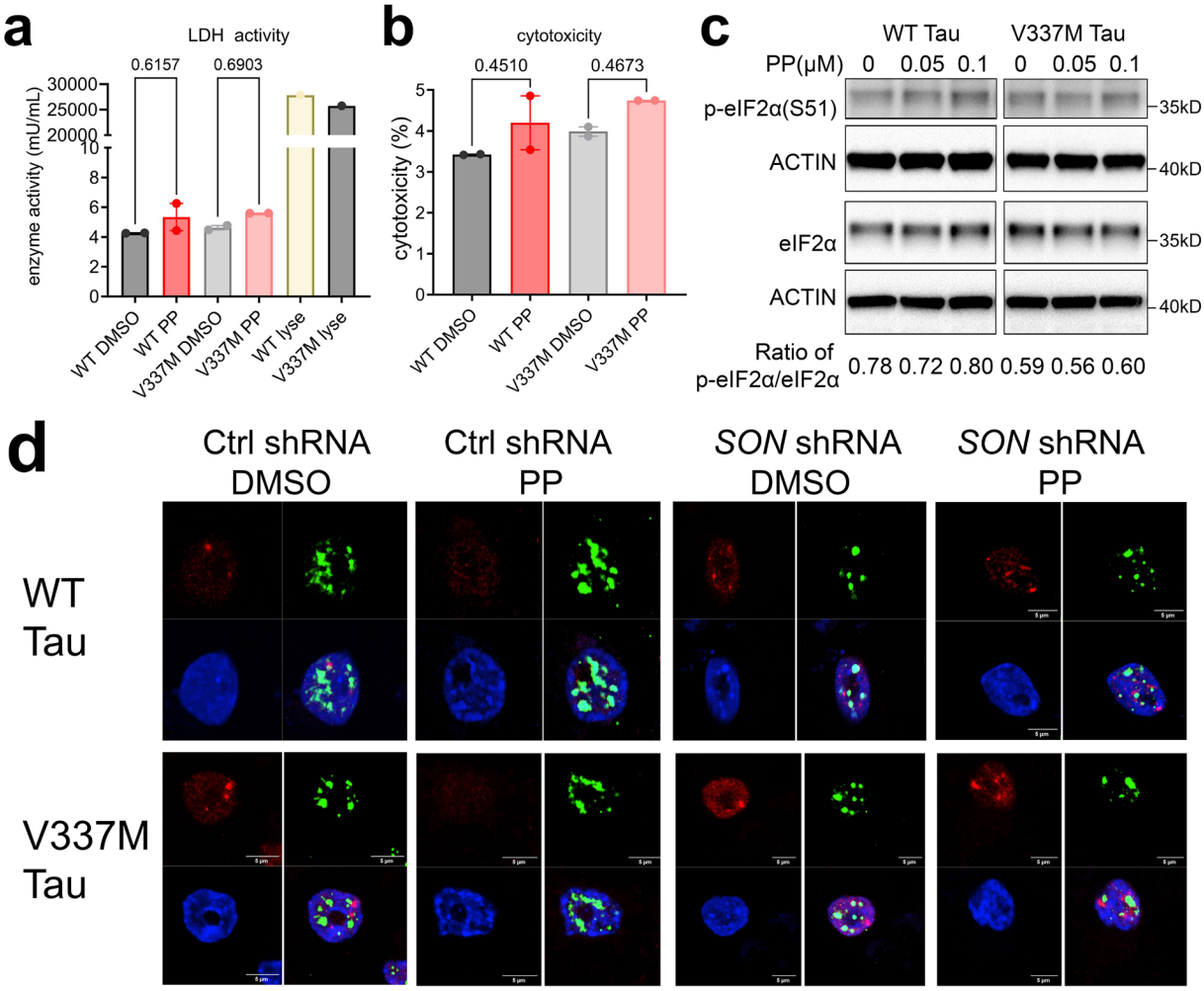

Supplementary Figure. 23. Nanomolar PP rejuvenates nuclear speckles and alleviates tau burden in human iPSC-neurons expressing mutant Tau in a SON-dependent manner without causing cellular stress. (**a-b**) WT and V337M Tau-expressing iPSC neurons were treated with 500 nM PP for 24 hours and LDH release assay were performed. LDH enzyme activity (**a**) and normalized cytotoxicity (**b**) were shown. (**c**) WT and V337M Tau-expressing iPSC neurons were treated with increasing concentration of PP for 12 hours and western blot of eIF2α and p-eIF2α were performed. The ratio of p-eIF2α to total eIF2α were calculated. (**d**) Wild-type and V337M Tau-expressing iPSC-neurons were infected with scrambled shRNA or SON shRNA-encoding lentivirus and treated with DMSO or PP (100nM) for 12 hours, and IF against nuclear speckle (Ab11826 against SRRM2), p-Tau (Ser422) and chromatin (DAPI) were performed.

Supplemental Movie legends:

Movie S1. Time lapse imaging of droplet formation with 20μm SON IDR1 in 125mM NaCl.

Movie S2. Time lapse imaging of droplet formation with 20μm SON IDR2 in 125mM NaCl.

Movie S3. Time lapse imaging of droplet formation with 20μm SRSF2 in 125mM NaCl.

Movie S4. Time lapse imaging of droplet formation with 10μm SON IDR2 supplemented with 0.6mg/ml GFP::SRSF2 MEF NE.